Two-channel Anderson impurity model: Single-electron Green's function, self-energies, and resistivity

Henrik Johannesson
Institute of Theoretical Physics, Chalmers University of Technology and Göteborg University, SE-412 96 Göteborg, Sweden

C. J. Bolech
Université de Genève, DPMC, 24 Quai Ernest Ansermet, CH-1211 Genève 4, Switzerland

Natan Andrei
Center for Materials Theory, Serin Physics Laboratory, Rutgers University, Piscataway, New Jersey 08854-8019, USA
(Received 20 November 2004; published 18 May 2005)

We compute exactly the low-energy single-electron Green's function, the impurity and electron self-energies, and the resistivity for the two-channel Anderson impurity model. These results are obtained by exploiting the boundary conformal field theory identified from the Bethe ansatz solution of the model. Using that solution we can make contact with the parameters of the original Hamiltonian and provide the detailed crossover between the two integer valence limits. Our results generalize those obtained previously in the context of the two-channel Kondo model.

DOI: 10.1103/PhysRevB.71.195107 PACS number(s): 71.27.+a, 75.20.Hr, 72.10.Fk, 73.23.−b

I. INTRODUCTION

Multichannel impurity physics is a well-established route to non-Fermi-liquid behavior. Its appeal is therefore understandable as an essential ingredient in many of the various theories that try to explain the unusual characteristics of numerous systems ranging from heavy fermions[1] to mesoscopic point contacts.[2] In this context, the two-channel Anderson impurity model occupies a central place. It was first introduced by Cox in an attempt to model the physics of certain U-based heavy fermions,[3] among which the compound UBe_{13} is a prime example. Following that line of thought, a dilute concentration of uranium in a $ThBe_{13}$ matrix will correspond to a metallic system with a feeble concentration of two-channel impurity centers. Impurity corrections to the different transport properties of that system should display fractional power laws indicative of non-Fermi-liquid behavior. For instance, corrections to the resistivity would display $\sqrt{T}$ dependence at low temperatures[4] and should constitute a particular experimentally accessible observable.

Indeed, transport measurements are good candidates for experiments, since they can also be performed in mesoscopic systems for which bulk thermodynamic measurements, possible for heavy fermions and other materials, are ineffectual. In this context, the two-channel Anderson model was already used successfully as the starting point of noncrossing approximation (NCA) calculations to model the temperature dependence of the differential conductance of Cu point contacts.[5,6]

The two-channel Anderson impurity model[7–9] describes the interaction of three-dimensional (3D) electrons with a local impurity carrying both spin and quadrupolar degrees of freedom. These degrees of freedom correspond to the lowest-energy configurations of a uranium impurity in charge states U^{4+} $(5f^2)$ and U^{3+} $(5f^3)$. Taking into account spin-orbit coupling and crystal-field splitting in a cubic background one ends up considering the minimal scenario of a (quadrupolar) Γ_3 doublet representation of the cubic group as the lowest-energy multiplet in U^{4+} and a Kramers doublet Γ_6 as the lowest-energy configuration in U^{3+}. These levels hybridize with those electrons from the conduction band effectuating the transition from one doublet to the other. Starting from the full electron field $\Psi(\vec{x})$, one carries out an expansion in harmonics corresponding to cubic symmetry, retaining only $\Psi_{\alpha\sigma}(r)$ which has the appropriate symmetry to couple to the impurity, with $\alpha=\pm$ denoting the quadrupolar degrees of freedom and $\sigma=\uparrow,\downarrow$ denoting magnetic (spin) degrees of freedom.

We then proceed to write the field in terms of 1D right (left) moving fields $\psi_{R\alpha\sigma}$ $(\psi_{L\alpha\sigma})$, representing the incoming (outgoing) radial components of the 3D electron fields that couple to the impurity,[7]

$$\Psi_{\alpha\sigma}(r) = \frac{i}{2\sqrt{2\pi r}}[e^{-ik_F r}\psi_{L\alpha\sigma}(r) - e^{ik_F r}\psi_{R\alpha\sigma}(r)], \qquad (1)$$

with a "free-electron" boundary condition $\psi_{L\alpha\sigma}(0)=\psi_{R\alpha\sigma}(0)$ imposed at the origin $r=0$.[10]

The Hamiltonian is then given by

$$H = H_{\text{bulk}} + H_{\text{ion}} + H_{\text{hybr}}, \qquad (2)$$

where

$$H_{\text{bulk}} = \int_0^\infty dr[:\psi^\dagger_{L\alpha\sigma}(r)(i\partial_r)\psi_{L\alpha\sigma}(r):-:\psi^\dagger_{R\alpha\sigma}(r)(i\partial_r)\psi_{R\alpha\sigma}(r):], \qquad (3)$$

$$H_{\text{ion}} = \epsilon_s f^\dagger_\sigma f_\sigma + \epsilon_q b^\dagger_{\bar{\alpha}} b_{\bar{\alpha}}, \qquad (4)$$

$$H_{\rm hybr} = V[\psi^\dagger_{L\alpha\sigma}(0) b^\dagger_{\bar{\alpha}} f_\sigma + f^\dagger_\sigma b_{\bar{\alpha}} \psi_{L\alpha\sigma}(0)]. \quad (5)$$

The conduction electrons here hybridize with the impurity via a matrix element V,[11] with the impurity modeled by a quadrupolar (magnetic) doublet of energy ϵ_q (ϵ_s), created by a boson (fermion) operator $b^\dagger_{\bar{\alpha}}$ ($f^\dagger_\sigma$).[12] Strong Coulomb repulsion implies single occupancy of the localized levels: $f^\dagger_\sigma f_\sigma + b^\dagger_{\bar{\alpha}} b_{\bar{\alpha}} = 1$. The free part of the Hamiltonian, $H_{\rm bulk}$, defines a linearized spectrum around the Fermi level. The Fermi velocity is set to unity, with the resulting 1D density of states $\rho = 1/(2\pi)$. Normal ordering is taken with respect to the filled Fermi sea.

The model in Eq. (2) was recently solved by two of us using a Bethe ansatz.[13] A complete description of spectrum and thermodynamics was given, and it was found that at low temperatures the theory is attracted to a line of fixed points parametrized by the impurity charge valence n_c (where $n_c = \langle f^\dagger_\sigma f_\sigma \rangle$ measures the average charge localized at the impurity site). Near integral charge valence $n_c \simeq 1$ ($n_c \simeq 0$) a magnetic (quadrupolar) moment forms at intermediate temperatures. This moment is then screened by the conduction electrons as the temperature is lowered, leading to a zero-temperature entropy $S_0^{\rm imp} = k_B \ln \sqrt{2}$ and impurity specific heat $C_{\rm v}^{\rm imp} \sim T \ln T$, typical of two-channel Kondo physics. In the mixed-valence regime one finds the same low-temperature behavior, but without the formation of a magnetic or quadrupolar moment at intermediate temperatures.

In previous work we constructed the boundary conformal field theory (BCFT), which describes the approach to criticality.[14] The leading scaling operators were identified—including the exactly marginal operator that generates the line of fixed points—and all physical scales and BCFT parameters were determined explicitly via a numerical fit to the exact solution in Ref. 13. This allowed us to go beyond the Bethe ansatz approach and derive the critical exponents of the Fermi edge singularities caused by time-dependent hybridization between conduction electrons and impurity. Our results challenged those obtained by more conventional, approximate schemes (see, e.g., Ref. 15).

In the present work we take the BCFT formulation one step further and extract the exact space- and time-dependent single-electron Green's function of the model. This allows us to calculate the self-energies of the conduction electrons and of the impurity, as well as the zero-temperature resistivity and leading temperature-dependent term.

The analysis is most easily performed by generalizing that of the multichannel Kondo model in Refs. 16 and 17. In fact, the very structure of the Green's function, as well as that of the leading terms of the resistivity, can be read off directly from the corresponding result for the two-channel Kondo model.[16,17] The only essential new element in the analysis is how to properly introduce the scales and amplitudes that determine the influence from the magnetic and quadrupolar degrees of freedom as one moves away from the integer valence limits.

In the next section we combine results from Ref. 14 and Refs. 16 and 17 to obtain the single-electron Green's function of the model. In Sec. III we use this result to derive the self-energy of the impurity, and in Sec. IV we report on the calculation of the resistivity. Section V contains a summary and a discussion of our results.

II. GREEN'S FUNCTION

At sufficiently low energies (or large distances) a quantum impurity interacting with conformal (i.e., linear dispersion) electrons can be represented by a conformally invariant boundary condition—this is the key idea of the BCFT formulation of a quantum impurity problem.[18] For the two-channel Anderson model, this boundary condition [which supersedes the trivial "free-electron" boundary condition $\psi_{L\alpha\sigma}(0) = \psi_{R\alpha\sigma}(0)$], is most easily described via a "gluing condition" on the charge, spin, and flavor conformal towers that make up its spectrum (for details, see Ref. 14). The dependence on the new boundary condition (*alias* the impurity) is picked up by the time-ordered left-right single-electron Green's functions

$$G_{LR}(\tau; r_1, r_2) = G^*_{RL}(\tau; r_1, r_2) \equiv \langle \psi_{L\alpha\sigma}(\tau, r_1) \psi^\dagger_{R\alpha\sigma}(0, r_2) \rangle \quad (6)$$

(with τ imaginary time) via the one-particle S-matrix

$$S_{(1)}(\omega_F) = {\rm e}^{2i\delta_F} C_{(1)}(\omega_F). \quad (7)$$

Here $C_{(1)}(\omega_F)$ is the amplitude for a single electron to scatter elastically off the impurity at the Fermi level ω_F, and $\delta_F = \delta(\omega_F)$ is the corresponding single-electron scattering phase shift. At large (mean) distances from the boundary, $|r_1 - r_2| \gg a$, with a some characteristic microscopic scale, one finds that[16]

$$G_{LR}(\tau; r_1, r_2) \sim \frac{S_{(1)}(\omega_F)}{\tau + i(r_1 + r_2)}. \quad (8)$$

Thus, at the level of the left-right Green's function, the boundary condition that emulates the presence of the impurity is coded by $S_{(1)}(\omega_F)$. In contrast, the large-distance left-left (LL) and right-right (RR) Green's functions $G_{mm}(\tau; r_1, r_2) \equiv \langle \psi_{m\alpha\sigma}(\tau, r_1) \psi^\dagger_{m\alpha\sigma}(0, r_2) \rangle$ with $m = L, R$ are insensitive to the particular boundary condition imposed:[16]

$$G_{LL}(\tau; r_1, r_2) = G^*_{RR}(\tau; r_1, r_2) \sim \frac{1}{\tau + i(r_1 - r_2)}, \quad |r_1 - r_2| \gg a. \quad (9)$$

Turning now to the the 3D electron field Green's function $\mathcal{G}(\tau, r_1, r_2) \equiv \langle \Psi_{\alpha\sigma}(\tau, r_1) \Psi^\dagger_{\alpha\sigma}(0, r_2) \rangle$ and expressing it in terms of the 1D propagators in Eqs. (8) and (9) one obtains

$$\begin{aligned} \mathcal{G}(\tau, r_1, r_2) = {} & {\rm e}^{-ik_F(r_1 - r_2)} G_{LL}(\tau, r_1, r_2) + {\rm e}^{ik_F(r_1 - r_2)} G_{RR}(\tau, r_1, r_2) \\ & + {\rm e}^{-ik_F(r_1 + r_2)} G_{LR}(\tau, r_1, r_2) + {\rm e}^{ik_F(r_1 + r_2)} G_{RL}(\tau, r_1, r_2). \end{aligned} \quad (10)$$

Continuing the 1D electron fields analytically to the full line $-\infty < r < \infty$ [with $\psi_{R\alpha\sigma}(\tau, r) = \psi_{L\alpha\sigma}(\tau, -r)$], averaging over impurity locations (thus restoring translational invariance), and exploiting a T-matrix formulation,[19] the Fourier-

transformed Green's function in Eq. (10) can be cast in the standard form

$$\mathcal{G}(\omega_n,k)=\frac{1}{i\omega_n-\epsilon_k-\Sigma(\omega_n)}, \tag{11}$$

with the self-energy $\Sigma(\omega_n)$ given by

$$\Sigma(\omega_n)=-in_i\frac{1-e^{2i\delta_F}C_1(\omega_F)}{2\pi g_F}\,\mathrm{sgn}(\omega_n). \tag{12}$$

Here n_i is the density of a dilute random distribution of impurities, g_F is the 3D "free-electron" density of states at the Fermi level, and $\mathrm{sgn}(\omega_n)$ is the sign function, with $\omega_n=2\pi(n+1/2)k_BT$, $n=0,\pm1,\pm2,\ldots$, Matsubara frequencies. In order to tie the self-energy $\Sigma(\omega_n)$ to the two-channel Anderson model in Eq. (2) we need to determine the *S*-matrix in Eq. (7) that is associated with the hybridization interaction in Eq. (5). The amplitude $C_{(1)}(\omega_F)$ can be determined in exact analogy with the two-channel Kondo problem in Ref. 16. Within the BCFT formalism $C_1(\omega_F)$ gets expressed as a certain combination of so-called "modular *S* matrices"[20]

$$S_{j_f}^{j_f'}=\frac{1}{\sqrt{2}}\sin[\pi(2j_f+1)(2j_f'+1)/4], \tag{13}$$

with structure and allowed values of the quantum numbers $j_f,j_f'=0,1/2,1$ determined by the $SU(2)_2$ Kac-Moody symmetry of the flavor sector.[14] Specifically,

$$C_1(\omega_F)=\frac{S_{1/2}^{1/2}S_0^0}{S_{1/2}^0S_0^{1/2}}, \tag{14}$$

and it follows from Eq. (13) that

$$C_1(\omega_F)=0. \tag{15}$$

Thus, the outgoing scattering state has no single-electron component after interaction with the impurity. This extreme non-Fermi-liquid behavior is the same as for the two-channel spin Kondo model[21] ($n_c=1$ limit of the two-channel Anderson model) and *is not modified as one moves into the mixed valence regime with* $n_c\neq0,1$. As seen from Eq. (7), the impurity valence n_c, connected to the phase shift δ_F via the Friedel-Langreth sum rule[22]

$$\delta_F=\frac{\pi}{4}n_c, \tag{16}$$

could only influence the scattering if there were a finite single-electron cross section at the Fermi level. However, as $C_1(\omega_F)=0$ independent of n_c, this does not happen. [Note that the phase shift δ_F is that of an electron with spin σ *and* flavor index α, hence the unconventional factor of $1/4$ in Eq. (16).[14]]

To summarize the analysis thus far: The zero-temperature single-electron Green's function is given by Eq. (10), with

$$\Sigma(\omega_n)=-in_i\frac{1}{2\pi g_F}\,\mathrm{sgn}(\omega_n), \tag{17}$$

where n_i and g_F are defined after Eq. (12). We should here stress that impurity-impurity interactions have been neglected in Eq. (17). As discussed in Ref. 16 this type of analysis is applicable only at temperatures high enough so that any remnant effects from interimpurity interactions are washed out (but low enough so that the theory is critical and the BCFT formulation remains valid). Also note that the expressions for the 1D propagators in Eqs. (8) and (9) pick up corrections when $|r_1-r_2|\leqslant a$,[23] implying that the result in Eqs. (11) and (17) gets modified when probing boundary correlations with large momenta.

To obtain the leading finite-temperature and frequency corrections to Eq. (17) we need to consider the theory slightly off the line of boundary fixed points. The scaling Hamiltonian H_{scaling} that governs the critical behavior close to the fixed line was identified in Ref. 14 as

$$H_{scaling}=H^*+\lambda_cJ(0)+\lambda_s\mathcal{O}^{(s)}(0)+\lambda_f\mathcal{O}^{(f)}(0)+\text{subleading terms}. \tag{18}$$

Here H^* is the critical Hamiltonian that represents H_{bulk} in Eq. (2), subject to the boundary condition that emulates the impurity terms H_{ion} and H_{hybr} in Eqs. (4) and (5), respectively. These terms, which break particle-hole symmetry, also give rise to the exactly marginal term $\lambda_cJ(0)$ in Eq. (18), with $J(0)=\Sigma_{\alpha,\sigma}:\psi_{\alpha\sigma}^\dagger\psi_{\alpha\sigma}(0):$ being the charge current at the impurity site and with λ_c its conjugate scaling field. This is the operator that generates the line of stable fixed points. *Off* the fixed line the terms H_{ion} and H_{hybr} allow for additional *irrelevant* boundary operators to enter the stage. Of these, $\lambda_s\mathcal{O}^{(s)}(0)$ and $\lambda_f\mathcal{O}^{(f)}(0)$, both of scaling dimension $\Delta=3/2$, are the leading ones. The spin boundary operator $\mathcal{O}^{(s)}(0)$ is the same operator that drives the critical behavior in the two-channel spin Kondo problem and is obtained by contracting the spin-1 field $\phi^{(s)}(0)$ with the vector of $SU(2)_2$ raising operators $\boldsymbol{J}_{-1}^{(s)}:\mathcal{O}^{(s)}(0)=\boldsymbol{J}_{-1}^{(s)}\cdot\boldsymbol{\phi}^{(s)}(0)$. The flavor boundary operator $\lambda_f\mathcal{O}^{(f)}(0)$ has the same structure. In obvious notation: $\mathcal{O}^{(f)}(0)=\boldsymbol{J}_{-1}^{(f)}\cdot\boldsymbol{\phi}^{(f)}(0)$.

In the case of the two-channel (spin) Kondo problem the flavor operator is effectively suppressed[10]: Of the two available energy scales, the *bandwidth D* and the *Kondo temperature* T_K [where T_K sets the scale for the crossover from weak coupling (high-temperature phase) to strong renormalized coupling (low-temperature phase)], only *D* enters the expression for the flavor scaling field λ_f. This is so since the Kondo temperature is dynamically generated in the spin sector (as indicated by the infrared divergences in perturbation theory) and hence cannot influence the scaling of the flavor degrees of freedom. On dimensional grounds one concludes that $\lambda_f\sim\mathcal{O}(1/\sqrt{D})$, whereas $\lambda_s\sim\mathcal{O}(1/\sqrt{T_K})$. For a small Kondo coupling, call it λ, $T_K\sim D\exp(-1/\lambda)\ll D$, and the critical behavior is therefore driven by $\mathcal{O}^{(s)}(0)$ alone. As we showed in Ref. 14, the picture for the two-channel Anderson model is more involved. There are here *two* dynamically generated temperature scales $T_{s,f}(\epsilon)$, both parametrized by $\epsilon=\epsilon_q-\epsilon_s$

and thus varying with the position on the fixed line via the dependence of the impurity valence n_c on ϵ.[13] The scaling fields $\lambda_{s,f}$ are parametrized accordingly[14]:

$$\lambda_{s,f} = \frac{B_{s,f}}{\sqrt{T_{s,f}}}, \tag{19}$$

with $B_{s,f}$ dimensionless constants. The precise dependence of $\lambda_{s,f}$ on ϵ was extracted in Ref. 14 from a fit to the numerical solution of the thermodynamic Bethe ansatz (TBA) equations of the model.[13] In the magnetic moment regime where $\epsilon \ll \mu - \Gamma$ [two-channel (spin) Kondo limit] $T_s \ll T_f$ and λ_s dominates. As ϵ increases T_s and T_f approach each other and become equal when $\epsilon = \mu$ (maximal mixed valence with no moment formation). Continuing along the fixed line, the two scales trade places, and eventually, at the quadrupolar critical end point ($\epsilon \gg \mu - \Gamma$) one finds that $T_s \gg T_f$. It follows that in the two-channel Anderson model *both* boundary operators $\mathcal{O}^{(s)}(0)$ and $\mathcal{O}^{(f)}(0)$ come into play, with their relative importance changing continuously as one moves along the fixed line.

Going back to the scaling Hamiltonian in Eq. (18), the effect of the exactly marginal term $\lambda_c J(0)$ is easily obtained via the observation that it samples the local charge at the impurity site, with the scaling field $\lambda_c = -n_c/4$ measuring the impurity valence per spin and flavor degree of freedom.[14] By the Friedel-Langreth sum rule in Eq. (16), the resulting shift of the charge content of the critical bulk Hamiltonian H^*, $Q \to Q - n_c$, shows up as a phase shift $\delta_F = \pi n_c/4$ on the electrons that scatter off the impurity charge potential at $r=0$. In other words, $\psi_{L\alpha\sigma} \to \exp(-i\pi n_c/4)\psi_{L\alpha\sigma}$ and $\psi_{R\alpha\sigma} \to \exp(i\pi n_c/4)\psi_{R\alpha\sigma}$, implying that the left-right propagators $G_{LR} = G^*_{RL}$ get phase shifted by $2\delta_F = \pi n_c/2$, as indicated in Eq. (8).

To probe the effects from the spin and flavor boundary operators in Eq. (18) requires a perturbative approach. Passing to a Lagrangian formalism, the correction δS to the Euclidean fixed point action due to $\mathcal{O}^{(f)}(0)$ and $\mathcal{O}^{(s)}(0)$ in Eq. (18) can be written as

$$\delta S = \sum_{k=f,s} \lambda_k \int_0^\beta d\tau' \boldsymbol{J}^{(k)}_{-1} \cdot \boldsymbol{\phi}^{(k)}(\tau', 0), \tag{20}$$

with $\beta = 1/k_B T$. To leading order in a perturbative expansion this leads to the following correction for the left-right propagator:

$$\delta_{\alpha\gamma}\delta_{\sigma\mu}\delta G(\tau; r_1, r_2) = \sum_{k=f,s} \lambda_k \int_0^\beta d\tau' \langle \psi_{L\alpha\sigma}(\tau, r_1) \boldsymbol{J}^{(k)}_{-1} \cdot \boldsymbol{\phi}^{(k)} \times (\tau', 0) \psi^\dagger_{R\gamma\mu}(0, r_2) \rangle_T. \tag{21}$$

The index T that appears in Eq. (21) refers to the "finite-T geometry" $\Gamma^+ = \{w = \tau + ir\}$, connected to the half-plane $\mathbb{C}^+ = \{\mathrm{Im}\, z > 0\}$ used at zero temperature via the conformal mapping $w = (\beta/\pi)\arctan(z)$.

The three-point functions in Eq. (21) are completely determined by conformal invariance up to multiplicative constants N_f and N_s (Ref. 16):

$$\delta G_{LR}(\tau, r_1, r_2) = i(\lambda_f N_f + \lambda_s N_s) e^{2i\delta_F} \left(\frac{\pi}{\beta}\right)^{7/2} \times \int_0^\beta d\tau' \frac{\left(-i \sin\frac{\pi}{\beta}[\tau + i(r_1 + r_2)]\right)^{3/2}}{\left(\sin\frac{\pi}{\beta}(\tau' - \tau - ir_1)\sin\frac{\pi}{\beta}(\tau' + ir_2)\right)^{5/2}}. \tag{22}$$

In the $n_c = 0$ (quadrupolar) limit where $\lambda_s \to 0$ and $\delta_F = 0$,[14] the theory is invariant under charge conjugation (particle-hole symmetry). Adapting an argument from Ref. 16 we may use this property to determine the phase of N_f, and together with an explicit calculation of $|N_f|^2$ one finds the value

$$N_f = 3/\sqrt{8}. \tag{23}$$

The value of N_s^2 is fixed via Eq. (23) by the vanishing of the four-point function[16]

$$\langle \psi^\dagger_{L\alpha\sigma}(\tau_1 + ir_1)\psi_{R\alpha\sigma}(\tau_1 - ir_1)\psi^\dagger_{L\gamma\mu}(\tau_2 + ir_2)\psi_{R\gamma\mu}(\tau_2 - ir_2)\rangle = (N_f^2 + N_s^2)(r_1 r_2)^{1/2} \frac{32}{9|\tau_1 - \tau_2|^3}, \tag{24}$$

and one concludes that

$$N_s = -i\frac{3}{\sqrt{8}}, \tag{25}$$

with the negative sign in Eq. (25) following from the condition that the expression for δG_{LR} in Eq. (22) collapses to that for the two-channel Kondo model[16] in the $n_c \to 1$ limit. The scaling fields λ_f and λ_s are the same as those that parametrize the thermodynamics and can thus be fitted to the exact TBA solution of the model[14] (see the next section). With this fit δG_{LR} in Eq. (22) will be completely specified. Note that by time reversal invariance, $\delta G_{RL} = \delta G^*_{LR}$.

Turning to the chiral propagators in Eq. (9), it is easy to verify that the corrections to these from δS vanish identically: $\delta G_{LL}(\delta G_{RR})$ is also given by the integral expression in Eq. (22) but with $r_2 \to -r_2 (r_1 \to -r_1)$. All zeros of the denominator are located in the upper (lower) half plane, and the integration contour can be deformed to Im $\tau \to -\infty(+\infty)$ without crossing any singularity; hence $\delta G_{LL} = \delta G_{RR} = 0$.

The integral expression for $\delta G_{LR} = \delta G^*_{RL}$ in Eq. (22) differs from that for the two-channel (spin) Kondo model in Ref. 16 only by having a prefactor $(\lambda_f - i\lambda_s)e^{i\pi n_c/2}$ instead of a single scaling field λ_s ($\equiv \lambda$ in Ref. 16). (It follows trivially that the result for the chiral propagators is the same for the two models.) From this point on we can therefore carry over the analysis intact from Ref. 16, at the end simply taking $\lambda \to (\lambda_f - i\lambda_s)e^{i\pi n_c/2}$. This gives, for the finite-temperature and frequency self-energy,[16]

$$\Sigma(\omega_n) = \frac{n_i \,\mathrm{sgn}(\omega_n)}{2\pi i g_F}\Bigg\{1 - \frac{3}{\sqrt{2}}(\lambda_f - i\lambda_s)e^{i(\pi/2)n_c}\left(\frac{2\pi}{\beta}\right)^{1/2} \times \int_0^1 du[u^{\beta|\omega_n|/2\pi}u^{-1/2}(1-u)^{1/2}F(u) - \Gamma^{-2}(3/2)u^{-1/2}(1-u)^{-3/2}]\Bigg\}, \tag{26}$$

where $F(u)$ is the hypergeometric function $F(3/2,3/2,1;u)$.

To summarize this section: to leading order in temperature and frequency, the exact single-electron Matsubara Green's function $\mathcal{G}(\omega_n,k)$ of the two-channel Anderson model for a dilute distribution of impurities is given by Eq. (10) with the self-energy $\Sigma(\omega_n)$ in Eq. (26). These are bulk-electron quantities; in the next section we make an aside to discuss their connection with the impurity response.

III. IMPURITY SELF-ENERGY

For the sake of simplicity, we will carry out this discussion at zero temperature. By analytic continuation to real frequencies,

$$\lim_{i\omega_n \to \omega + i0^+} \Sigma(\omega_n) = \Sigma^R(\omega), \tag{27}$$

one obtains from Eq. (26) an integral expression for the retarded electron self-energy $\Sigma^R(\omega)$. By taking the $T \to 0$ limit and approximating the integral as done in Ref. 16 one finds that[24]

$$\Sigma^R_{T=0}(\omega) = \frac{n_i}{2\pi i g_F}\Bigg[1 + \frac{12}{\sqrt{\pi}}(\mathcal{A}_1 + i\mathcal{A}_2) \times [1 - i\,\mathrm{sgn}(\omega)]\,|\omega|^{1/2}\Bigg], \tag{28}$$

with

$$\begin{cases} \mathcal{A}_1(\lambda_f,\lambda_s,n_c) \equiv \lambda_f \cos(n_c\pi/2) + \lambda_s \sin(n_c\pi/2), \\ \mathcal{A}_2(\lambda_f,\lambda_s,n_c) \equiv \lambda_f \sin(n_c\pi/2) - \lambda_s \cos(n_c\pi/2). \end{cases} \tag{29}$$

Writing down the relevant equations of motion, one can make a connection between the self-energy in Eq. (28) and the impurity Green's function.[25] Defining the latter one following the same conventions as in Ref. 26, the relation reads

$$\Sigma^R(\omega) = n_i \frac{V^2}{2\pi g_F} G^R_{imp}. \tag{30}$$

Parametrizing the impurity Green's function with a spectral weight equal to $1/2$, a hybridization amplitude[14] $\Gamma \equiv \pi\rho V^2$, and a self-energy $\Sigma^R_{imp}(\omega)$, we can extract

$$\Sigma^R_{imp}(\omega) = \omega - \epsilon + i\Gamma\left(1 - \frac{n_i}{2\pi i g_F}[\Sigma^R(\omega)]^{-1}\right). \tag{31}$$

The resulting formula for the impurity self-energy inherits from $\Sigma^R(\omega)$ a range of validity for $|\omega| \ll T_K$, where $T_K \equiv 4\Gamma/\pi^2 e^{-(\pi/2)|\epsilon|/\Gamma}$ is the two-channel Kondo temperature.[13]

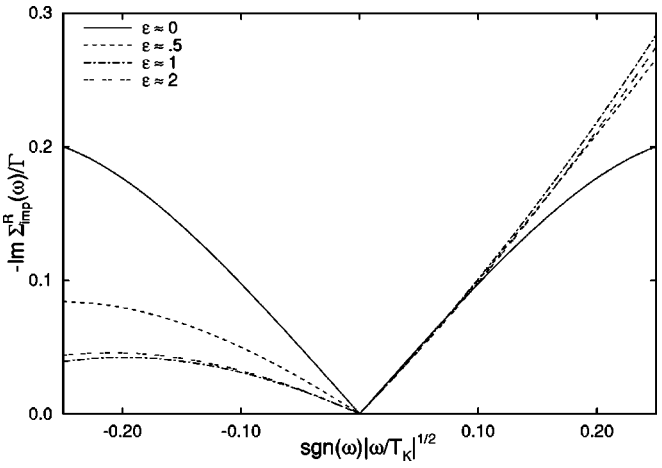

FIG. 1. Imaginary part of the zero-temperature impurity self-energy as a function of frequency. Different curves correspond to different values of the impurity configurational energy splitting (ϵ). The frequencies are scaled with the Kondo temperature T_K.

In Fig. 1 we show the imaginary part of the retarded impurity self-energy as a function of frequency (scaled with the Kondo temperature) for different values of the energy splitting ϵ. Only the curves for positive values of this parameter are shown in the figure, since for negative values one simply has to use the relation $\mathrm{Im}\,\Sigma^R_{imp}(\omega,-\epsilon) = \mathrm{Im}\,\Sigma^R_{imp}(-\omega,\epsilon)$ to obtain the corresponding curves. These results are in fair agreement with the ones obtained recently using the numerical renormalization group (NRG) method.[26] Additionally, notice that the figure required knowledge of $\mathcal{A}_1$ and $\mathcal{A}_2$ as functions of ε; we shall comment on this in the next section.

IV. RESISTIVITY

Given the retarded electron self-energy $\Sigma^R(\omega)$, defined by Eqs. (26) and (27), one can readily obtain the resistivity $\rho(T)$ of the model to leading order in temperature. Adapting the argument in Appendix C of Ref. 16, the assumption that the impurity-electron interaction is well described using the two-channel s-wave decomposition in Eq. (1) implies that the resistivity can be expressed directly in terms of $\mathrm{Im}\,\Sigma^R(\omega)$. From Eqs. (26) and (27) one obtains

$$\mathrm{Im}\,\Sigma^R(\omega) = -\frac{n_i}{2\pi g_F}\Bigg\{1 - 3\left(\frac{\pi}{\beta}\right)^{1/2}\Bigg[\mathcal{A}_1(\lambda_f,\lambda_s,n_c) \times \int_0^1 du\{\cos[\beta\omega(\ln u)/2\pi]u^{-1/2}(1-u)^{1/2}F(u) - \Gamma^{-2}(3/2)u^{-1/2}(1-u)^{-3/2}\} + \mathcal{A}_2(\lambda_f,\lambda_s,n_c) \times \int_0^1 du\,\sin[\beta\omega(\ln u)/2\pi]u^{-1/2}(1-u)^{1/2}F(u)\Bigg]\Bigg\}, \tag{32}$$

We have here used the property that $u^{\beta|\omega_n|/2\pi}\,\mathrm{sgn}(\omega_n)$

$\rightarrow \cos[(\beta\omega/2\pi)\ln u] - i\sin[(\beta\omega/2\pi)\ln u]$ under the analytic continuation $i\omega_n \rightarrow \omega + i0^+$.

As shown in Ref. 25 for this class of problems, vertex corrections to the resistivity involve *s*-wave correlations which vanish identically. It follows that the Kubo formula for the resistivity contains only the quasiparticle lifetime τ, with no weighting over large-angle scattering processes. With *two* local orbital channels ($\alpha = \pm$) of charge conduction, the Kubo formula thus reads[19]

$$\rho^{-1}(T) = \frac{4e^2}{3m_e}\int \frac{d^3k}{(2\pi)^3}\left[-\frac{dn_F(\epsilon_k)}{d\epsilon_k}\right]k^2\tau(\epsilon_k). \tag{33}$$

Here e and m_e are the electron charge and mass, respectively, $n_F(\epsilon_k)$ is the Fermi distribution function, and $\tau(\epsilon_k)$ is the lifetime of a quasiparticle of energy $\epsilon_k = k^2/2m_e$,

$$\tau(\epsilon_k) = -\frac{1}{2}[\mathrm{Im}\,\Sigma^R(\epsilon_k)]^{-1}. \tag{34}$$

Combining Eqs. (32)–(34), it follows that

$$\begin{aligned}\rho^{-1}(T) = \frac{4\pi(eg_F v_F)^2}{3n_i}\Bigg\{1 + 3\left(\frac{\pi}{\beta}\right)^{1/2}\int_{-\infty}^{\infty}\frac{dx}{4\cosh^2(x/2)} \\ \times\Bigg[\mathcal{A}_1(\lambda_f,\lambda_s,n_c)\int_0^1 du\{\cos[x(\ln u)/2\pi]u^{-1/2} \\ \times(1-u)^{1/2}F(u) - \Gamma^{-2}(3/2)u^{-1/2}(1-u)^{-3/2}\} \\ + \mathcal{A}_2(\lambda_f,\lambda_s,n_c)\int_0^1 du\{\sin[x(\ln u)/2\pi]u^{-1/2} \\ \times(1-u)^{1/2}F(u)\}\Bigg]\Bigg\},\end{aligned} \tag{35}$$

where $x \equiv \epsilon_k/k_BT$. We have here used that $[dn_F/d\epsilon_k]$ in Eq. (33) rapidly goes to zero away from the Fermi level, allowing us to approximate the momenta that appear in the integral by k_F ($=m_e v_F$). (Note that previously v_F was set to unity. We still use units where $\hbar = 1$.) Carrying out the integrals over x and subsequently over u (this second integral has to be done numerically, but to machine accuracy the result is found to be a rational number and expected to be exact),[16] one finally obtains, for the low-temperature resistivity,

$$\rho(T) = \rho(0)\left[1 + 4\left(\frac{\pi}{\beta}\right)^{1/2}\mathcal{A}_1(\lambda_f,\lambda_s,n_c)\right], \tag{36}$$

with

$$\rho(0) = \frac{3n_i}{4\pi(eg_F v_F)^2}. \tag{37}$$

Since both λ_f and λ_s on the one hand[14] and n_c on the other hand[13] are known to be functions of ϵ, the expression for the leading low-temperature dependence is related to the original impurity Hamiltonian via this single parameter.

This behavior is illustrated in Fig. 2. While we have plotted the curves over the full interval $0 \leqslant T \leqslant T_K$, we should alert the reader that our results are exact only in the scaling regime $T \ll T_K$. The explicit connection between $\lambda_{f,s}$ and ϵ was obtained from a fit of the low-temperature thermodynamics to the results of the TBA solution.[14] But the thermodynamics involves only the squares of the scaling fields and the sign remains therefore undetermined. However, in the limit of integer valence we have

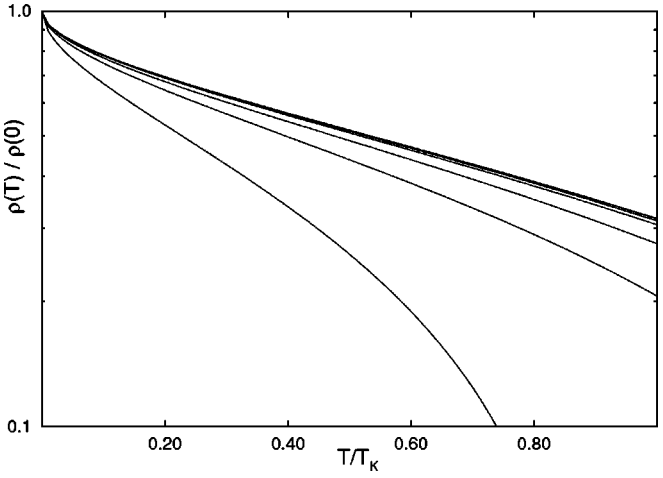

FIG. 2. Resistivity vs temperature curves for different values of the microscopic Hamiltonian parameter ϵ. Positive and negative values of ϵ fall on top of each other; from left to right the curves correspond to $|\epsilon| \simeq 0.0$, 0.5, 0.8, 1.1, 1.4, 1.8, and 2.1. The curves corresponding to the last two values of ϵ fall on top of each other in the scale of the figure, which illustrates the collapse into a universal curve as the system goes away from mixed valence.

$$\lim_{\epsilon/\Gamma \rightarrow \pm\infty}\mathcal{A}_1(\lambda_f(\epsilon),\lambda_s(\epsilon),n_c(\epsilon)) = \lambda_{f,s}(\epsilon), \tag{38}$$

and in that limit the model maps onto the weak-coupling two-channel Kondo model ($J_K < J^*$, with J^* the Kondo fixed point under renormalization to low energies) for which the sign of $\lambda_{f,s}(\epsilon)$ is known to be negative (it is expected to reverse sign for $J_K > J^*$).[16] Since the combined BCFT and TBA analysis indicates that the scaling fields vary continuously and do not change sign, we conclude that the coefficient $\mathcal{A}_1$ is always negative. Hence, the resistivity is a monotonically decreasing function of temperature for all values of ϵ. In the case of n_c, the Bethe ansatz solution provides directly an expression that relates it to ϵ.[13]

With these considerations the values of $\mathcal{A}_{1,2}(\varepsilon)$ are completely determined, which allowed us in the previous section to plot the impurity self-energy. It is interesting to point out that a positive sign for the scaling fields ($\lambda_{f,s}$) will hamper the comparison of that plot with the NRG results. Moreover, a positive sign will spoil the causal properties of the self-energy and is therefore unphysical for the Anderson model (even in the mixed-valence regime).

Away from $\epsilon \approx 0$, we can use Eq. (19) and our results of Ref. 14 to derive an approximate expression for the resistivity that highlights its scaling properties,

$$\rho(T)/\rho(0) = 1 - \frac{\sqrt{4\pi}}{3}[\cos(n_c\pi/2) + \sin(n_c\pi/2)]\sqrt{\frac{T}{T_K}}. \tag{39}$$

Here $T_K = \min\{T_f, T_s\}$ is the BCFT Kondo scale and the prefactors are in correspondence with the precise definition of

this scale as given in our previous work. It is important to remark again that the asymptotic expansion for small temperatures is valid only for $T \ll T_K$. For consistency, the same definition of the Kondo scale[13] was used for both plots in Figs. 1 and 2 (the prefactors in the definition are of course not universal and depend on the particular convention).

It is here interesting to discuss the experimentally measured low-T resistivity of the thoriated UBe_{13} compound, mentioned in the Introduction, which shows a $\sqrt{T}$ behavior but with a positive coefficient. As discussed in Refs. 4 and 27, this would imply that in the (single-impurity) Kondo model framework this system exhibits a strong electron-impurity coupling ($J_K > J^*$). It was speculated that such a regime was achievable near mixed valence in the context of the (single-impurity) two-channel Anderson model (see Ref. 7 for a review). Our results, however, do not support those ideas. Perhaps, since $U_{1-x}Th_xBe_{13}$ with $x=0.1$ is far from the dilute limit, lattice effects might play a role in reversing the sign of that coefficient. While later measurements on the same compound have confirmed the $\sqrt{T}$ behavior with a positive coefficient,[28] on the other hand, a $\sqrt{T}$ scaling of the resistivity with a negative coefficient has been recently observed in a different uranium-based heavy-fermion material $Sc_{1-x}U_xPd_3$ (but only for large dopings, $x \approx 0.35$,[29] when a single-impurity description of the low-temperature physics is not always expected).

V. SUMMARY AND DISCUSSION

In a previous article[14] we presented the technical details of the BCFT solution of the two-channel Anderson model and discussed its asymptotic low-temperature thermodynamics. In that context we were able to make the connection with the full solution obtained using the thermodynamic Bethe ansatz formalism and could explicitly match the scaling fields with the microscopic parameters of the lattice Hamiltonian. Here we completed the task by calculating dynamical- and transport-related quantities (the single-electron Green's function, the electron and impurity self-energies, and the resistivity). Using our previous results from Ref. 14, these quantities are parametrized directly in terms of the energy difference between impurity configurations in the original Hamiltonian (ϵ). We have shown, in particular, how our analytic expression for the impurity self-energy captures the low-frequency behavior in agreement with the results of other nonperturbative techniques like Wilson's numerical renormalization group method.[26] As we mentioned in the Introduction, having reliable access to transport quantities is of crucial importance for the comparison and interpretation of experiments that continue to seek indisputable realizations of multichannel Kondo physics. The work presented here furthers our understanding of two-channel Kondo physics in mixed-valent scenarios, thus widening the range of possible candidate systems for experimental realizations.

ACKNOWLEDGMENTS

We would like to thank F. B. Anders for discussions about his recent NRG results for this model and for useful correspondence. H.J. acknowledges support from the Swedish Research Council. C.J.B. was partially suported by the MaNEP initiative of the Swiss National Science Foundation.

[1] A. Hewson, *The Kondo Problem to Heavy Fermions* (Cambridge University Press, Cambridge, England, 1993).
[2] L. P. Kouwenhoven, D. G. Austing, and S. Tarucha, Rep. Prog. Phys. **64**, 701 (2001).
[3] D. L. Cox, Phys. Rev. Lett. **59**, 1240 (1987); **61**, 1527(E) (1988).
[4] F. G. Aliev, S. Viera, R. Villar, J. L. Martinez, C. L. Seaman, and M. B. Maple, Physica B **206–207**, 454 (1995).
[5] M. H. Hettler, J. Kroha, and S. Hershfield, Phys. Rev. Lett. **73**, 1967 (1994).
[6] M. H. Hettler, J. Kroha, and S. Hershfield, Phys. Rev. B **58**, 5649 (1998).
[7] For a review, see D. L. Cox and A. Zawadowski, Adv. Phys. **47**, 599 (1998).
[8] A. Schiller, F. B. Anders, and D. L. Cox, Phys. Rev. Lett. **81**, 3235 (1998).
[9] J. Kroha and P. Wölfle, Acta Phys. Pol. B **29**, 3781 (1998).
[10] I. Affleck and A. W. W. Ludwig, Nucl. Phys. B **360**, 641 (1991).
[11] As follows from the decomposition in Eq. (1), the hybridization matrix element V in Eq. (5) is related to the original 3D matrix element, V' call it, by $V=(k_F^2/2\pi^2)V'$.
[12] While indices α and σ transform according to the corresponding fundamental representations of SU (2), the overbar on the index $\bar{\alpha}$ indicates that it transforms instead according to the complex conjugate representation.
[13] C. J. Bolech and N. Andrei, Phys. Rev. Lett. **88**, 237206 (2002); see also Phys. Rev. B **71**, 205104 (2005).
[14] H. Johannesson, N. Andrei, and C. J. Bolech, Phys. Rev. B **68**, 075112 (2003); J. Magn. Magn. Mater. **272–276**, e103 (2004).
[15] D. L. Cox and A. E. Ruckenstein, Phys. Rev. Lett. **71**, 1613 (1993).
[16] I. Affleck and A. W. W. Ludwig, Phys. Rev. B **48**, 7297 (1993).
[17] A. W. W. Ludwig and I. Affleck, Nucl. Phys. B **428**, 545 (1994).
[18] For a review, see I. Affleck, Acta Phys. Pol. B **26**, 1869 (1995).
[19] G. D. Mahan, *Many-Particle Physics* (Plenum, New York, 1981).
[20] P. Di Francesco, P. Mathieu, and D. Senechal, *Conformal Field Theory* (Springer-Verlag, New York, 1997).
[21] Note that for the multichannel (spin) Kondo model the amplitude $C_{(1)}$ gets expressed in terms of modular S-matrices in the *spin* sector (Ref. 16). The same construction is possible also for the two-channel Anderson model, but this requires a redefinition of the charge quantum numbers of the model, implying in particular that $n_c \to 1-n_c$. In this manifestly particle-hole symmetric formulation of the Kondo limit one has that $C_{(1)}=S_{(1)}$. For details, see Ref. 14.
[22] D. C. Langreth, Phys. Rev. **150**, 516 (1966).
[23] A. E. Mattsson, S. Eggert, and H. Johannesson, Phys. Rev. B **56**, 15615 (1997).

[24] In the appropriate limits this expression reduces to the one for the two-channel Kondo model presented in Ref. 16. Note, however, the misprint in the relevant Eqs. (1.10) and (3.59) of that reference.
[25] N. E. Bickers, D. L. Cox, and J. W. Wilkins, Phys. Rev. B **36**, 2036 (1987).
[26] F. B. Anders, Phys. Rev. B **71**, 121101 (2005).
[27] F. G. Aliev, H. El Mfrarrej, S. Vieira, R. Villar, and J. L. Martinez, Europhys. Lett. **32**, 765 (1995).
[28] R. P. Dickey, M. C. de Andrade, J. Herrmann, M. B. Maple, F. G. Aliev, and R. Villar, Phys. Rev. B **56**, 11169 (1997).
[29] R. P. Dickey, V. S. Zapf, P. C. Ho, E. J. Freeman, N. A. Frederick, and M. B. Maple, Phys. Rev. B **68**, 104404 (2003).